Cancer Screening and Prevention **2026** | Epub
DOI: 10.14218/CSP.2026.00017

Original Article

Multidimensional Pan-cancer Analysis of NAT10: Cancer-type-specific Clinical and Biological Associations and Prognostic Potential

Yuan Ding[1,2], Lihua Ren[1,2] and Ruihua Shi[1,2*]

[1]*Department of Gastroenterology, Zhongda Hospital, Southeast University, Nanjing, Jiangsu, China;* [2]*School of Medicine, Southeast University, Nanjing, Jiangsu, China*

Received: August 14, 2026 | **Revised:** September 14, 2026 | **Accepted:** October 06, 2026 | **Published online:** October 30, 2026

Abstract

Background and objectives: N-acetyltransferase 10 (NAT10), a major RNA acetyltransferase mediating N4-acetylcytidine modification, has been implicated in cancer progression. We examined its cancer-type-specific associations with clinical outcomes, genomic features, and tumor immune characteristics.

Methods: We analyzed public TCGA and GTEx datasets using UCSC Xena and complementary resources, including GEPIA2, HPA, cBioPortal, TIMER2.0, STRING, LinkedOmics, and CancerSEA. Analyses included NAT10 expression, pathological stage, survival, genomic alterations, immune-cell infiltration, stemness, and molecular pathways. Exploratory immune-checkpoint-blockade (ICB) survival analyses used Kaplan–Meier Plotter cohorts receiving anti-PD-1 (n = 411), anti-PD-L1 (n = 459), or anti-CTLA-4 (n = 112).

Results: *NAT10* expression was elevated in multiple cancer types and was associated with adverse survival in selected malignancies. Higher *NAT10* expression correlated positively with estimated myeloid-derived suppressor cell and cancer-associated fibroblast infiltration and negatively with several T-cell and natural killer-cell populations. *NAT10*-associated genes were enriched in RNA-processing pathways. In exploratory ICB cohorts, higher *NAT10* expression was nominally associated with longer overall survival following anti-PD-1 therapy (hazard ratio (HR) = 0.68, 95% confidence interval (CI): 0.52–0.90) and anti-PD-L1 therapy (HR = 0.72, 95% CI: 0.56–0.92), but not anti-CTLA-4 therapy (HR = 0.66, 95% CI: 0.39–1.11).

Conclusions: *NAT10* shows cancer-type-dependent prognostic, molecular, and immune associations. Its associations with survival after ICB are exploratory and require independent clinical and mechanistic validation.

Introduction

N4-acetylcytidine (ac4C) is an evolutionarily conserved RNA modification involved in the regulation of RNA stability, translation efficiency, and cellular homeostasis.[1-3] N-acetyltransferase 10 (NAT10), a major acetyltransferase responsible for ac4C modification, has increasingly been implicated in cancer development and progression.[1,4] Aberrant NAT10 activity has been associated with diverse tumor-related processes, including RNA metabolism, cell proliferation, DNA damage responses, ferroptosis, and therapeutic resistance.[5,6] These observations raise the possibility that the biological and clinical relevance of NAT10 may differ substantially among cancer types.[7,8]

The *NAT10* gene encodes an acetyltransferase involved in RNA modification processes.[9,10] RNA modifications represent an important layer of post-transcriptional regulation that can influence RNA stability, processing, localization, and translation.[2,3,11] NAT10-mediated ac4C modification has been reported to affect RNA stability and translational efficiency, thereby influencing multiple cellular processes relevant to tumor biology.[1,12] Previous studies have demonstrated cancer-promoting roles of NAT10 in individual tumor types, including colon and bladder cancer.[5,6] Mechanistically, cancer-specific studies have linked NAT10 to

Keywords: NAT10; ac4C; Pan-cancer; Tumor microenvironment; Prognosis; Immune-checkpoint blockade; Bioinformatics.
***Correspondence to:** Ruihua Shi, Department of Gastroenterology, Zhongda Hospital, Southeast University, Nanjing, Jiangsu 210009, China. ORCID: https://orcid.org/0000-0003-4977-8801. Tel: +86-025-83262835, Fax: +86-025-83262835, E-mail: ruihuashi@126.com
How to cite this article: Ding Y, Ren L, Shi R. Multidimensional Pan-cancer Analysis of NAT10: Cancer-type-specific Clinical and Biological Associations and Prognostic Potential. *Cancer Screen Prev*. Published online: Oct 30, 2026. DOI: 10.14218/CSP.2026.00017.

© 2026 The Author(s). This article has been published under the terms of Creative Commons Attribution-Noncommercial 4.0 International License (CC BY-NC 4.0), which permits noncommercial unrestricted use, distribution, and reproduction in any medium, provided that the following statement is provided. "This article has been published in *Cancer Screening and Prevention* at https://doi.org/10.14218/CSP.2026.00017 and can also be viewed on the Journal's website at https://www.xiahepublishing.com/journal/csp".

suppression of ferroptosis and enhanced tumor progression in colorectal cancer, DNA-repair-associated chemoresistance in bladder cancer, and regulation of tumor–immune interactions in several malignancies.[13,14] More recent evidence has also implicated NAT10-mediated RNA acetylation in metastatic and metabolic programs in individual tumor contexts, highlighting substantial context dependency in NAT10 function.[8] A previous pan-cancer study also described the expression, prognostic relevance, and immune-infiltration characteristics of NAT10 across multiple malignancies.[7] Therefore, the present study was not designed merely to reproduce these observations. Instead, we sought to extend previous work by integrating multiple complementary dimensions, including pathological stage, genomic alterations, RNA-modification-related features, tumor stemness, immune-regulatory programs, single-cell functional states, and survival associations in publicly available immune-checkpoint-blockade cohorts.[15] Particular emphasis was placed on identifying cancer-type-dependent heterogeneity and on distinguishing exploratory treatment-associated associations from established predictive biomarkers.[16] However, the cancer-type-specific relationships among *NAT10* expression, genomic features, immune characteristics, and immunotherapy-associated outcomes remain incompletely characterized.[13] To further evaluate the role of NAT10 in cancer, we performed an integrated analysis of data from multiple databases, including The Cancer Genome Atlas (TCGA), the Genotype-Tissue Expression Project (GTEx), cBioPortal, and the Human Protein Atlas (HPA). This analysis explored the expression patterns of NAT10 and its correlations with patient survival, immune checkpoints, tumor stemness scores, prognostic value, immune modulators, genomic features, immune characteristics, and functional enrichment. Through this systematic investigation, this study aimed to characterize the cancer-type-specific clinical, genomic, and immunological associations of NAT10 and to evaluate its potential prognostic relevance.

Materials and methods

An overview of the study design, data sources, analysis-specific inclusion and exclusion criteria, and analytical workflow is provided in Supplementary Fig. 1. A summary of the publicly available cohorts, data sources, sample sizes where available, and analysis-specific eligibility criteria is provided in Supplementary Table. 1. TCGA and GTEx were sources of cohort-level expression data. The UCSC Xena Toil RNA-seq Recompute hub hosts a harmonized expression matrix derived from TCGA, TARGET, and GTEx and does not represent an independent patient cohort. GEPIA2, TIMER2.0, cBioPortal, HPA, STRING, LinkedOmics, CancerSEA, and other named resources were used for data access, visualization, annotation, or complementary analyses as specified below.

NAT10 expression analysis

NAT10 messenger RNA (mRNA) expression levels in normal human tissues were investigated using the HPA database.[17] Additionally, representative immunohistochemistry and immunofluorescence images of NAT10 in normal or tumor tissues and cells were retrieved from the HPA database. TIMER2.0 was used to assess the expression levels of the *NAT10* gene in a diverse range of cancer tissues.[18] For the expression data of NAT10 from normal and tumor samples, the TCGA and GTEx databases were employed.[19,20] The HPA (https://www.proteinatlas.org/), TIMER2.0 (http://timer.cistrome.org/), TCGA (https://portal.gdc.cancer.gov/), and GTEx (https://gtexportal.org/) databases were accessed for the corresponding expression and protein-level analyses. HPA immunohistochemistry and immunofluorescence images were used for qualitative visualization only, and no quantitative image analysis was performed. Because TCGA and GTEx data were generated from distinct cohorts, comparisons integrating the two resources may remain susceptible to residual technical and cohort-related differences despite the harmonized expression data provided by the analytical platforms. Accordingly, TCGA–GTEx comparisons were interpreted as cross-dataset expression comparisons rather than as matched case-control experiments.

Pathological stage analysis

In our study, the "Stage plot" function within the Gene Expression Profiling Interactive Analysis database (GEPIA2; http://gepia.cancer-pku.cn/) was utilized to explore the association between *NAT10* expression and pathological stage.[21] The uniformly processed TCGA TARGET GTEx pan-cancer RNA-sequencing dataset (PANCAN, N = 19,131, G = 60,499) was obtained from the UCSC Xena Toil RNA-seq Recompute hub.[22] In this matrix, gene expression values are RSEM-normalized transcripts per million (TPM) values provided as log2(TPM + 0.001). *NAT10* expression values were extracted directly from the downloaded matrix, and no additional logarithmic transformation was applied. Cancer cohorts with fewer than three available samples were excluded from this analysis. This process ultimately yielded expression data for 30 cancer cohorts. Differences in *NAT10* expression across pathological-stage groups within each cancer cohort were evaluated using R software (version 3.6.4). For pairwise comparisons, an unpaired Student's t test was employed. For comparisons involving more than two pathological-stage groups, analysis of variance was used.

Prognostic analysis

GEPIA2 was used to obtain the overall survival (OS) and disease-free survival significance maps and NAT10 survival plots across all TCGA tumors. The cutoff-high (50%) and cutoff-low (50%) values were set as the expression thresholds to divide the samples into high- and low-*NAT10*-expression cohorts, corresponding to a median-expression-based stratification. Survival distributions between the high- and low-*NAT10*-expression groups were compared using the log-rank test. For the complementary pan-cancer survival analysis, the same UCSC Xena Toil RNA-seq Recompute dataset (dataset ID: TcgaTargetGtex_rsem_gene_tpm; version: 2016-09-03) was used. Gene expression values in this matrix are RSEM-normalized TPM values already provided as log2(TPM + 0.001); therefore, no additional logarithmic transformation was performed. *NAT10* expression data were matched with the corresponding survival information. Samples lacking the required survival information or with follow-up times shorter than 30 days were excluded from the corresponding survival analysis. Moreover, cancer cohorts with fewer than 10 samples per cohort were removed from the analysis. After this preprocessing, expression data for 44 cancer cohorts, along with the corresponding overall survival data for the samples, were obtained. To examine the association between gene expression and

 DOI: 10.14218/CSP.2026.00017 | 2026

survival in each cancer type, the R package survival (version 3.2-7) was utilized. The coxph function was employed to construct a Cox proportional hazards regression model. Hazard ratios (HRs) and corresponding 95% confidence intervals (CIs) were estimated from the Cox proportional hazards regression models. Differences in survival distributions were evaluated using the log-rank test. The Cox models used in this pan-cancer screening analysis were univariable models based on *NAT10* expression and did not include multivariable adjustment for clinicopathological covariates.

Immune-regulatory gene, immune checkpoints, and tumor stemness score analysis

Data obtained from the UCSC Xena database were used to analyze the associations between *NAT10* expression and 150 immune-regulatory genes classified as chemokines (41 genes), receptors (18 genes), major histocompatibility complex-related genes (21 genes), immunoinhibitors (24 genes), and immunostimulators (46 genes). For each sample in the pan-cancer dataset obtained from UCSC Xena, *NAT10* expression and the expression of 60 immune-checkpoint-related genes, including 24 inhibitory and 36 stimulatory genes, were retrieved. Pearson correlation coefficients were then calculated between the expression of the *NAT10* gene and these immune pathway marker genes. Furthermore, the association between *NAT10* expression and the DNA methylation-based stemness score (DNAss) was evaluated across cancer types. Pearson correlation analysis was performed to assess the relationship between *NAT10* expression and DNAss.

Immune infiltration analysis

We retrieved the expression data of the *NAT10* gene from each sample within the pan-cancer dataset downloaded from the UCSC Xena database. Subsequently, the gene expression profile of each tumor was extracted, and this profile was mapped to GeneSymbol. The ESTIMATE package in R was then used.[23] Based on the gene expression data, stromal scores, immune scores, and ESTIMATE scores were calculated for each sample within each cancer type. The resulting ImmuneScore, StromalScore, and ESTIMATEScore were obtained for subsequent correlation analyses. To assess the relationships between *NAT10* expression and ESTIMATE-derived ImmuneScore, StromalScore, and ESTIMATEScore, the corr.test function of the R package psych (version 2.1.6) was used to calculate Pearson correlation coefficients. In addition, TIMER2.0 was used to evaluate the associations between *NAT10* expression and estimated immune-cell infiltration across TCGA cancer types.

NAT10-related gene analysis

The STRING database (https://cn.string-db.org/) was utilized to retrieve experimentally determined NAT10-binding proteins specific to *Homo sapiens*.[24] Subsequently, the "Similar Gene Detection" module in GEPIA2 was used to identify the top 100 genes most strongly associated with *NAT10* expression. Next, TIMER2.0 was used to evaluate Spearman correlations between *NAT10* expression and the top 10 NAT10-associated genes across cancer types. These correlations were presented as a heatmap. Finally, the Sangerbox 3.0 database (http://sangerbox.com/home.html) was accessed to obtain KEGG pathways and Gene Ontology (GO) terms associated with the NAT10-interacting and correlated genes.[25]

Genetic alteration analysis

The mutational characteristics of NAT10 in various cancers were analyzed using the cBioPortal tool (http://www.cbioportal.org/).[26] Additionally, cBioPortal was employed to further investigate the types and frequencies of *NAT10* gene mutations across all tumors. Data from the same UCSC Xena Toil RNA-seq Recompute dataset (TcgaTargetGtex_rsem_gene_tpm) were used to extract *NAT10* expression together with the expression of 44 RNA modification-related genes, comprising 10 m1A-related, 13 m5C-related, and 21 m6A-related genes. Because the expression matrix was already provided as log2(TPM + 0.001), no additional logarithmic transformation was performed. Pearson correlation analysis was subsequently performed between *NAT10* expression and the 44 RNA-modification-related genes. Somatic mutation data generated using the MuTect2 pipeline were obtained from the TCGA-level Simple Nucleotide Variation dataset. The tumor mutational burden (TMB) of each tumor was calculated from the TCGA somatic mutation data using the R package maftools.[27] Finally, the TMB and gene expression data of the samples were integrated.

Functional and enrichment analyses

Associations between *NAT10* expression and 14 cancer functional states were explored using single-cell transcriptomic data available through CancerSEA (http://biocc.hrbmu.edu.cn/CancerSEA/home.jsp).[28] Subsequently, gene co-expression analysis of NAT10 was carried out via the LinkedOmics website (https://www.linkedomics.org/login.php).[29] To determine the correlation between NAT10 and co-expressed genes, Pearson's correlation analysis was employed to evaluate the association between *NAT10* expression and the co-expressed genes. Functional enrichment of NAT10-associated genes in breast invasive carcinoma (BRCA) and esophageal carcinoma (ESCA) was further evaluated using gene set enrichment analysis, including KEGG pathways and GO biological-process terms. Normalized enrichment scores and false-discovery-rate values were used to summarize the enrichment results, as shown in Figures 1f–g and 2c–d. BRCA and ESCA were selected for exploratory cancer-specific analyses because NAT10 was significantly upregulated in both cancer types in the pan-cancer expression analysis and complementary public data were available for additional molecular characterization, including mutation profiling, protein-level visualization, and co-expression/enrichment analyses. For ESCA, CancerSEA additionally provided single-cell functional-state information.

Immunotherapy analysis

The Kaplan–Meier Plotter database (https://kmplot.com/analysis/) was utilized to analyze the association between *NAT10* expression and survival outcomes in patients receiving immune checkpoint blockade (ICB).[30] Patients receiving anti-PD-1, anti-PD-L1, or anti-CTLA-4 therapy were analyzed according to the treatment categories available in the Kaplan–Meier Plotter immunotherapy module. OS was used as the survival endpoint. Analyses were performed using the Kaplan–Meier Plotter Immunotherapy v.2023 dataset. The evaluable sample sizes were 933 for the no-immunotherapy cohort, 411 for any anti-PD-1 therapy (nivolumab, N = 173; pembrolizumab, N = 238), 459 for any anti-PD-L1 therapy

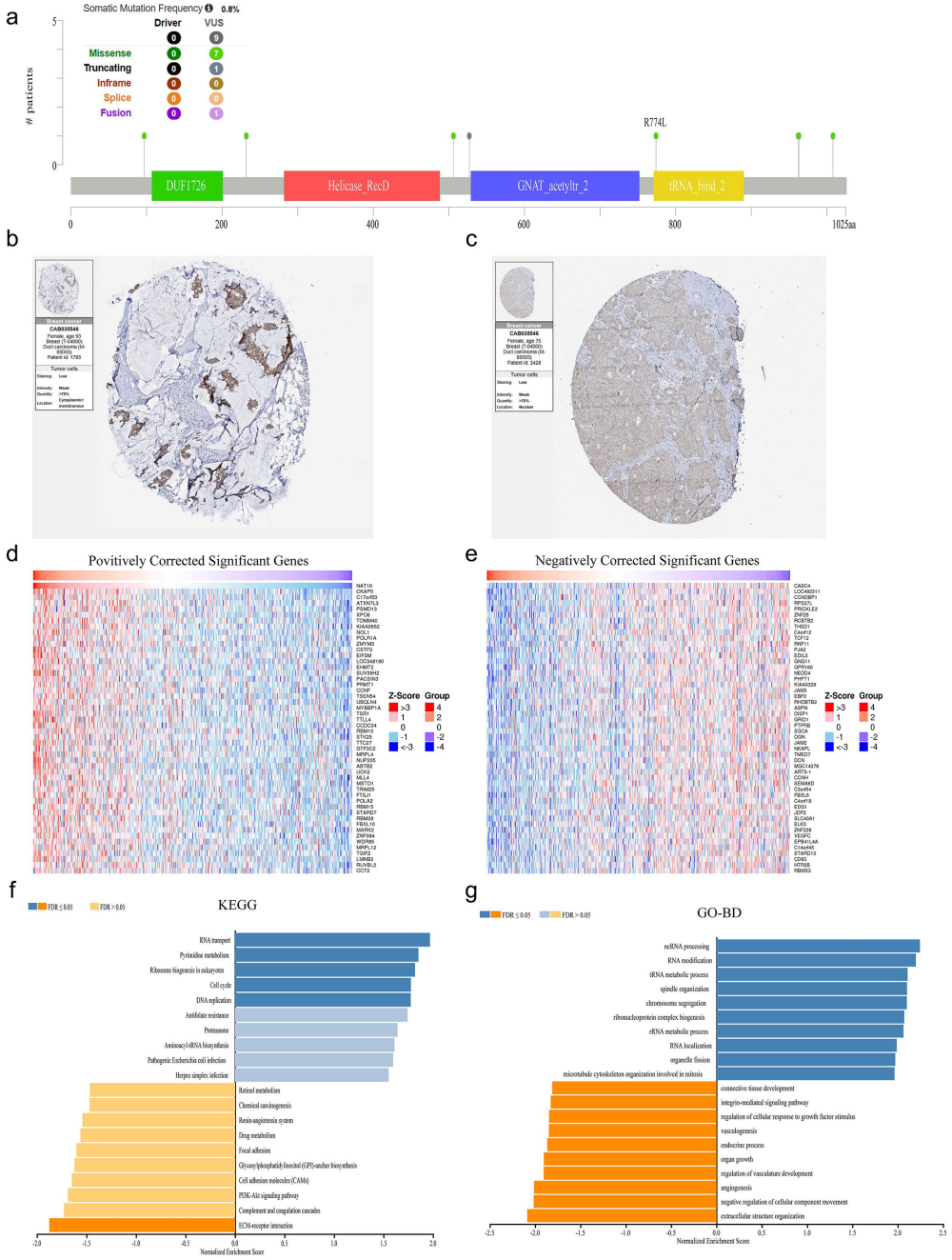


Fig. 1. Molecular and functional characterization of NAT10 in breast invasive carcinoma (BRCA). (a) Distribution of *NAT10* somatic mutations across the NAT10 protein sequence in BRCA, showing mutation types, locations, and numbers of affected cases. (b–c) Representative HPA immunohistochemical images illustrating NAT10 protein staining in breast cancer tissues. (d) Heatmap of the top 50 genes positively correlated with *NAT10* expression in BRCA. (e) Heatmap of the top 50 genes negatively correlated with *NAT10* expression in BRCA. (f) Gene set enrichment analysis of KEGG pathways associated with *NAT10* co-expression in BRCA; positive and negative normalized enrichment scores are shown, with FDR significance indicated. (g) Gene set enrichment analysis of Gene Ontology biological-process terms associated with *NAT10* co-expression in BRCA. Image credit: Human Protein Atlas (https://www.proteinatlas.org/). aa, amino acids; BP, biological process; CAMs, cell adhesion molecules; DUF1726, domain of unknown function 1726; ECM, extracellular matrix; FDR, false discovery rate; GNAT, Gcn5-related N-acetyltransferase; GO, Gene Ontology; GPI, glycosylphosphatidylinositol; HPA, Human Protein Atlas; KEGG, Kyoto Encyclopedia of Genes and Genomes; NAT10, N-acetyltransferase 10; PI3K, phosphoinositide 3-kinase; RecD, recombination protein D; rRNA, ribosomal RNA; tRNA, transfer RNA; VUS, variant of uncertain significance.

 DOI: 10.14218/CSP.2026.00017 | 2026

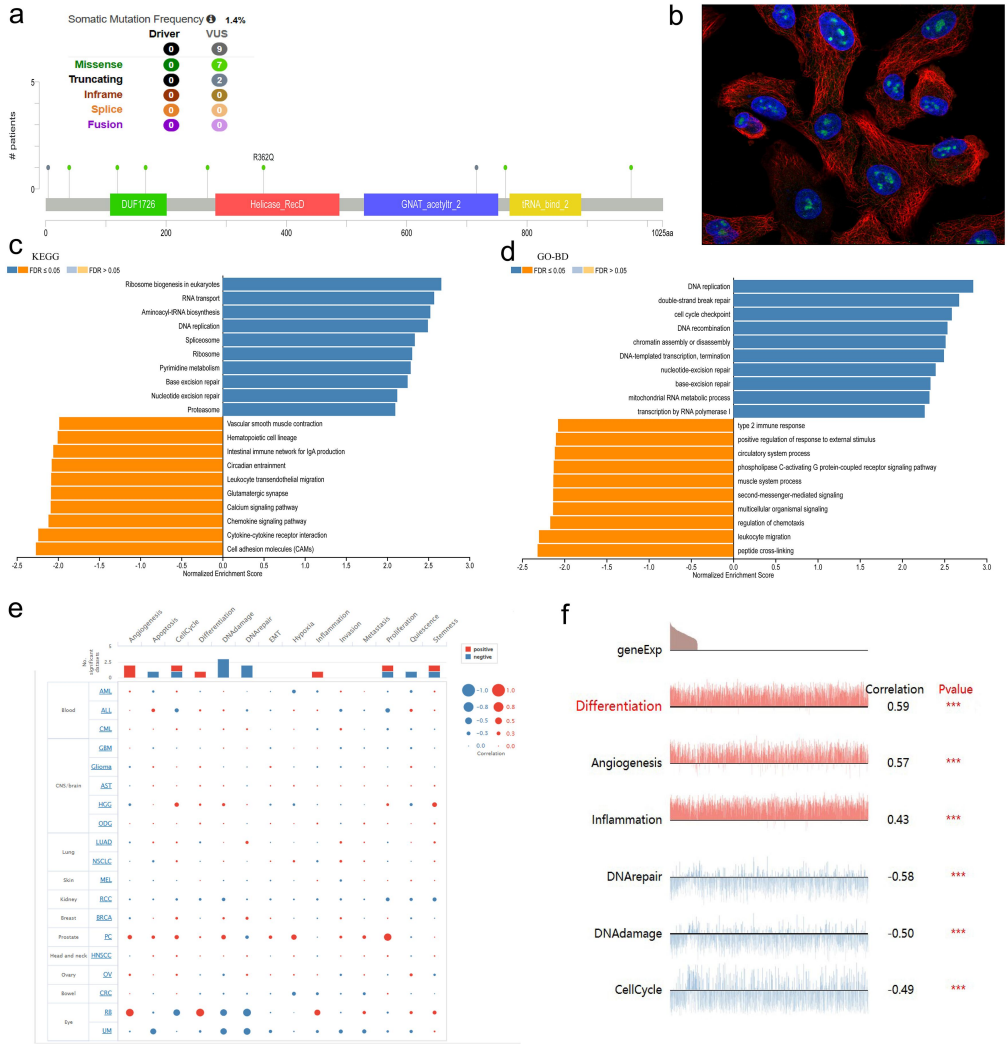


Fig. 2. Molecular and functional characterization of NAT10 in ESCA. (a) Distribution of *NAT10* somatic mutations across the NAT10 protein sequence in ESCA, showing mutation types, locations, and numbers of affected cases. (b) Representative HPA immunofluorescence image illustrating the subcellular localization of NAT10. (c) Gene set enrichment analysis of KEGG pathways associated with *NAT10* co-expression in ESCA. (d) Gene set enrichment analysis of Gene Ontology biological-process terms associated with *NAT10* co-expression in ESCA. (e) CancerSEA analysis of correlations between *NAT10* expression and 14 functional states across single-cell cancer datasets. (f) Correlations between *NAT10* expression and functional states in the ESCA single-cell dataset, showing positive associations with differentiation, angiogenesis, and inflammation and negative associations with DNA repair, DNA damage, and cell cycle. ***$P < 0.001$. Image credit: Human Protein Atlas (https://www.proteinatlas.org/). aa, amino acids; ALL, acute lymphoblastic leukemia; AML, acute myeloid leukemia; AST, astrocytoma; BP, biological process; BRCA, breast invasive carcinoma; CAMs, cell adhesion molecules; CML, chronic myeloid leukemia; CNS, central nervous system; CRC, colorectal cancer; DUF1726, domain of unknown function 1726; EMT, epithelial–mesenchymal transition; ESCA, esophageal carcinoma; FDR, false discovery rate; GBM, glioblastoma multiforme; GNAT, Gcn5-related N-acetyltransferase; GO, Gene Ontology; HGG, high-grade glioma; HNSCC, head and neck squamous cell carcinoma; HPA, Human Protein Atlas; KEGG, Kyoto Encyclopedia of Genes and Genomes; LUAD, lung adenocarcinoma; MEL, melanoma; NAT10, N-acetyltransferase 10; NSCLC, non-small cell lung cancer; ODG, oligodendroglioma; OV, ovarian serous cystadenocarcinoma; PC, prostate cancer; RB, retinoblastoma; RCC, renal cell carcinoma; RecD, recombination protein D; tRNA, transfer RNA; UM, uveal melanoma; VUS, variant of uncertain significance.

(atezolizumab, $N = 447$; durvalumab, $N = 12$), and 112 for any anti-CTLA-4 therapy (ipilimumab, $N = 112$). The Kaplan–Meier Plotter immunotherapy database was accessed in September 2026. Patients were stratified into high- and low-*NAT10*-expression groups using the "auto select best cutoff" option of Kaplan–Meier Plotter, which evaluates possible cutoff values between the lower and upper quartiles and selects the best-performing threshold. HRs with 95% CIs were recorded where available. The *P* values generated by Kaplan–Meier Plotter were nominal and were not adjusted for multiple comparisons. Given the heterogeneity of the publicly available immunotherapy cohorts, this analysis was considered exploratory.

Statistical analysis

Statistical analyses were performed using R software. Continuous variables between two independent groups were compared using the Wilcoxon rank-sum test unless otherwise specified. For comparisons involving more than two groups, the Kruskal–Wallis test was used. Correlations between *NAT10* expression and continuous molecular or immune-related variables were evaluated using Pearson's or Spearman's correlation analysis, as specified for each analysis. Survival outcomes were evaluated using Kaplan–Meier analysis and the log-rank test, and HRs with 95% CIs were estimated using Cox proportional hazards regression models. For analyses involving simultaneous testing across multiple cancer types or predefined gene panels, unadjusted *P* values were corrected using the Benjamini–Hochberg false-discovery-rate procedure. A false discovery rate (FDR)-adjusted *P* value < 0.05 was considered statistically significant for these multiple-comparison analyses. Analyses performed through external web-based platforms were interpreted according to the statistical outputs provided by the corresponding platform, and nominal *P* values are explicitly identified where multiple-testing-adjusted values were not available. All statistical tests were two-sided. A nominal *P* value < 0.05 was considered statistically significant for individual hypothesis tests, whereas an FDR-adjusted *P* value < 0.05 was considered statistically significant for analyses involving multiple testing. Statistical tests and significance thresholds are specified in the corresponding Methods subsections and figure legends where available.

Results

NAT10 upregulation in multiple human cancers

We first evaluated the mRNA levels of NAT10 in normal human tissues. NAT10 was expressed in most tissues and showed a broad tissue-expression pattern, suggesting that its expression is not restricted to a specific tissue type (Fig. 3a). Subsequently, we delved into the expression of NAT10 in various tumors. By examining the TCGA and GTEx databases, we investigated the expression changes of NAT10 between tumor tissues and their corresponding normal tissues. The mRNA expression of NAT10 was significantly higher in multiple cancer types, including glioblastoma multiforme (GBM), glioma (GBMLGG), brain lower grade glioma (LGG), uterine corpus endometrial carcinoma (UCEC), breast invasive carcinoma, lung adenocarcinoma (LUAD), ESCA, stomach and esophageal carcinoma (STES), kidney renal papillary cell carcinoma (KIRP), pan-kidney cohort (KIPAN), colon adenocarcinoma (COAD), colon adenocarcinoma/rectum adenocarcinoma (COADREAD), stomach adenocarcinoma (STAD), head and neck squamous cell carcinoma (HNSC), kidney renal clear cell carcinoma (KIRC), lung squamous cell carcinoma (LUSC), liver hepatocellular carcinoma (LIHC), high-risk wilms tumor (WT), bladder urothelial carcinoma (BLCA), rectum adenocarcinoma (READ), pancreatic adenocarcinoma (PAAD), testicular germ cell tumors (TGCT), uterine carcinosarcoma (UCS), acute lymphoblastic leukemia (ALL), acute myeloid leukemia (LAML), kidney chromophobe (KICH), and cholangiocarcinoma (CHOL). Conversely, the mRNA expression of NAT10 was significantly downregulated in prostate adenocarcinoma (PRAD), thyroid carcinoma (THCA), ovarian serous cystadenocarcinoma (OV), and adrenocortical carcinoma (ACC). In other tumors, no significant differences in *NAT10* expression were observed, as shown in Figure 3b and c. Collectively, these results demonstrate that *NAT10* expression is dysregulated across multiple malignancies, although both the direction and magnitude of the expression difference vary among cancer types.

Association of NAT10 expression with pathological stage and prognosis across cancers

We explored *NAT10* expression across different pathological stages. Significant stage-associated differences in *NAT10* expression were observed in KIRP, LIHC, LUAD, and PAAD (Fig. 4a–d). Subsequently, we conducted a more detailed analysis of the expression of NAT10 in different tumor pathological stages using the UCSC Xena database. The results further demonstrated significant stage-associated differences in *NAT10* expression in LUAD, KIRP, the pan-kidney cohort (KIPAN), LIHC, and PAAD (Fig. 4e). Collectively, these results demonstrate stage-associated variation in *NAT10* expression in selected cancer types.

Furthermore, when comparing high- and low-NAT10-expression cohorts, elevated *NAT10* expression was associated with shorter OS in multiple tumor types, such as adrenocortical carcinoma (ACC), head and neck squamous cell carcinoma (HNSC), kidney chromophobe (KICH), kidney renal papillary cell carcinoma (KIRP), liver hepatocellular carcinoma (LIHC), and uveal melanoma (UVM) (Fig. 5a–g). Likewise, a comparison between high- and low-NAT10 - expression cohorts demonstrated that increased *NAT10* expression was associated with decreased disease-free survival in ACC, cervical squamous cell carcinoma and endocervical adenocarcinoma (CESC), diffuse large B - cell lymphoma (DLBC), HNSC, LIHC, and pancreatic adenocarcinoma (PAAD) (Fig. 5h–n). Using the UCSC Xena pan-cancer dataset, we additionally examined the association between *NAT10* expression and overall survival across available tumor cohorts. Because the dataset contains cohorts derived from different projects, including TCGA and TARGET, these results were interpreted as a complementary pan-cancer screening analysis rather than as an independent TCGA validation. We observed that higher *NAT10* expression was associated with poorer overall survival in nine cohorts, including TARGET-LAML, TCGA-KIPAN, TCGA-HNSC, TCGA-GBM, TCGA-LIHC, TCGA-UVM, TCGA-LAML, TCGA-ACC, and TCGA-KICH (Fig. 5o). Collectively, these analyses indicate that higher *NAT10* expression is associated with unfavorable survival outcomes in selected cancer types, while its prognostic association is not uniform across all malignancies.

Association between NAT10 expression and immunomodulatory genes

We next investigated the associations between *NAT10* expression and tumor immune characteristics, including immunomodulatory genes, immune checkpoints, tumor stemness scores, and immune infiltration. Initially, from the pan-cancer dataset downloaded from the UCSC Xena database, we extracted the *NAT10* gene and 150 marker genes belonging to five immune pathways: chemokine (41 markers), receptor (18 markers), major histocompatibility complex (21 markers), immunoinhibitor (24 markers), and immunostimulator (46 markers). Subsequently, the expression

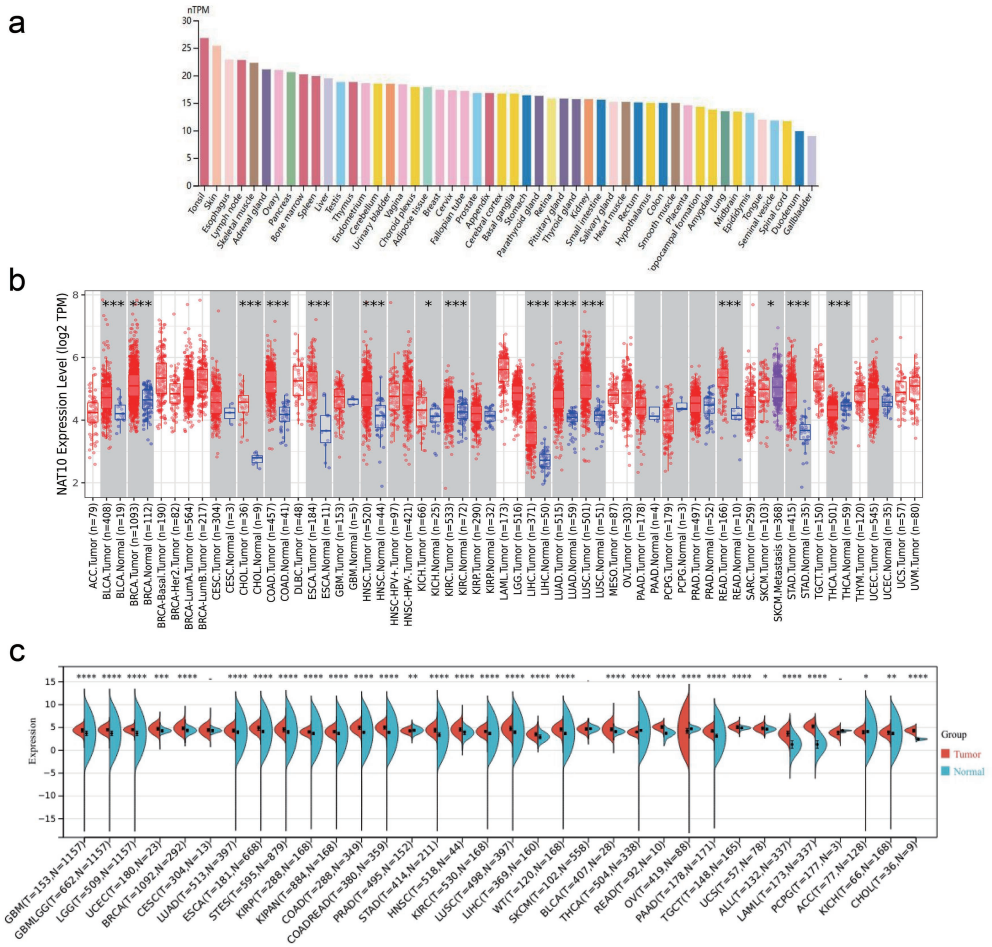


Fig. 3. Pan-cancer expression profile of NAT10. (a) *NAT10* mRNA expression levels across normal human tissues based on the Human Protein Atlas (HPA). (b) Comparison of *NAT10* expression between tumor and adjacent normal tissues across TCGA cancer types. (c) Comparison of *NAT10* expression between tumor and normal tissues using integrated TCGA and GTEx data, displayed as split violin plots. Statistical significance is indicated in the corresponding panels. ACC, adrenocortical carcinoma; ALL, acute lymphoblastic leukemia; BLCA, bladder urothelial carcinoma; BRCA, breast invasive carcinoma; CESC, cervical squamous cell carcinoma and endocervical adenocarcinoma; CHOL, cholangiocarcinoma; COAD, colon adenocarcinoma; COADREAD, combined colon and rectum adenocarcinoma cohort; DLBC, diffuse large B-cell lymphoma; ESCA, esophageal carcinoma; GBM, glioblastoma multiforme; GBMLGG, combined glioblastoma and lower-grade glioma cohort; GTEx, Genotype-Tissue Expression; HER2, human epidermal growth factor receptor 2; HNSC, head and neck squamous cell carcinoma; HPV, human papillomavirus; KICH, kidney chromophobe; KIPAN, pan-kidney cohort; KIRC, kidney renal clear cell carcinoma; KIRP, kidney renal papillary cell carcinoma; LAML, acute myeloid leukemia; LGG, brain lower-grade glioma; LIHC, liver hepatocellular carcinoma; LUAD, lung adenocarcinoma; LumA, luminal A; LumB, luminal B; LUSC, lung squamous cell carcinoma; MESO, mesothelioma; mRNA, messenger RNA; NAT10, N-acetyltransferase 10; nTPM, normalized transcripts per million; OV, ovarian serous cystadenocarcinoma; PAAD, pancreatic adenocarcinoma; PCPG, pheochromocytoma and paraganglioma; PRAD, prostate adenocarcinoma; READ, rectum adenocarcinoma; SARC, sarcoma; SKCM, skin cutaneous melanoma; STAD, stomach adenocarcinoma; STES, combined stomach and esophageal carcinoma cohort; TCGA, The Cancer Genome Atlas; TGCT, testicular germ cell tumors; THCA, thyroid carcinoma; THYM, thymoma; TPM, transcripts per million; UCEC, uterine corpus endometrial carcinoma; UCS, uterine carcinosarcoma; UVM, uveal melanoma; WT, Wilms tumor.

data of these marker genes in each sample were further screened, and Pearson correlations between *NAT10* expression and immune-pathway marker gene expression were calculated. The results showed that the expression of NAT10 was positively correlated with most immunomodulatory genes (Fig. 6a). Next, we analyzed the correlations between NAT10 and specific immune checkpoints, namely the inhibitory (24 markers) and stimulatory (36 markers) ones. Based on the data, *NAT10* expression was significantly correlated with multiple inhibitory and stimulatory immune-checkpoint genes across cancer types (Fig. 6b). Furthermore, *NAT10* expression was significantly correlated with the DNAss in 13 cancer types. Specifically, in these 13 tumors, including STES (stomach and esophageal carcinoma), SARC (sarcoma), KIRP (kidney renal papillary cell carcinoma), KIPAN (pan-kidney cohort), STAD (stomach adenocarcinoma), PRAD (prostate adenocarcinoma), HNSC (head and neck squamous cell car-

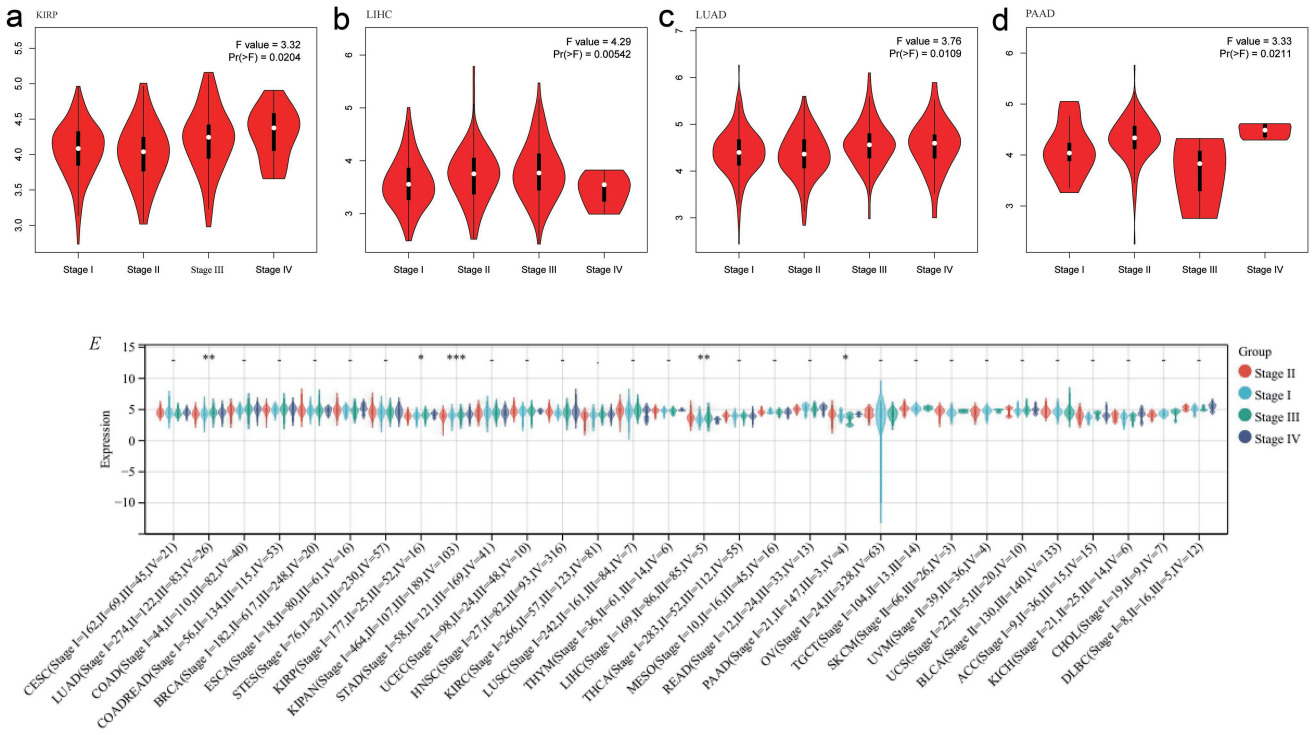


Fig. 4. Association between *NAT10* expression and pathological stage across cancer types. *NAT10* expression across pathological stages in kidney renal papillary cell carcinoma (KIRP) (a), liver hepatocellular carcinoma (LIHC) (b), lung adenocarcinoma (LUAD) (c), and pancreatic adenocarcinoma (PAAD) (d). (e) Pan-cancer comparison of *NAT10* expression across pathological stages in the UCSC Xena dataset. ACC, adrenocortical carcinoma; BLCA, bladder urothelial carcinoma; BRCA, breast invasive carcinoma; CESC, cervical squamous cell carcinoma and endocervical adenocarcinoma; CHOL, cholangiocarcinoma; COAD, colon adenocarcinoma; COADREAD, combined colon and rectum adenocarcinoma cohort; DLBC, diffuse large B-cell lymphoma; ESCA, esophageal carcinoma; HNSC, head and neck squamous cell carcinoma; KICH, kidney chromophobe; KIPAN, pan-kidney cohort; KIRC, kidney renal clear cell carcinoma; LUSC, lung squamous cell carcinoma; MESO, mesothelioma; NAT10, N-acetyltransferase 10; OV, ovarian serous cystadenocarcinoma; READ, rectum adenocarcinoma; SKCM, skin cutaneous melanoma; STAD, stomach adenocarcinoma; STES, combined stomach and esophageal carcinoma cohort; TGCT, testicular germ cell tumors; THCA, thyroid carcinoma; THYM, thymoma; UCEC, uterine corpus endometrial carcinoma; UCS, uterine carcinosarcoma; UCSC, University of California, Santa Cruz; UVM, uveal melanoma.

cinoma), LUSC (lung squamous cell carcinoma), THCA (thyroid carcinoma), TGCT (testicular germ cell tumors), PCPG (pheochromocytoma and paraganglioma), UVM (uveal melanoma), and UCS (uterine carcinosarcoma), a significant positive correlation was observed (Fig. 6c).

Furthermore, significant associations were observed between *NAT10* expression and ESTIMATE-derived stromal scores across multiple cancer types. Specifically, negative correlations were observed in GBM, GBMLGG, LGG, UCEC, BRCA, CESC, LUAD, ESCA, STES, SARC, KIRP, COAD, COADREAD, STAD, LUSC, THYM, LIHC, TARGET-WT, and SKCM-P, whereas positive correlations were observed in LAML, KIPAN, and UVM (Fig. 7a–v). Subsequently, we utilized TIMER2 to explore the relationship between *NAT10* expression and the infiltration levels of various immune cells across all TCGA-profiled cancers. Our study employed multiple algorithms, including xCell, TIMER, CIBERSORT, CIBERSORT-ABS, QUANTISEQ, MCP-counter, EPIC, and TIDE, to evaluate the associations between *NAT10* expression and immune-cell infiltration. The findings indicated a positive association between the infiltration levels of neutrophils, cancer-associated fibroblasts, and myeloid-derived suppressor cells, while a negative correlation was observed between the infiltration levels of T cells, natural killer (NK) cells, endothelial cells, and *NAT10* expression in multiple tumors (Fig. 7w). Together, these findings demonstrate cancer-type-dependent associations between *NAT10* mRNA expression and multiple components of the tumor immune microenvironment.

NAT10-related gene analysis

We utilized the online tool STRING to obtain 50 NAT10-binding proteins, as shown in Fig. 8a. Subsequently, GEPIA2 was used to identify the top 100 genes most strongly associated with *NAT10* expression. Among these, the top 10 NAT10-associated genes showed predominantly positive expression correlations with NAT10 across multiple cancer types (Fig. 8b). Following this, we conducted KEGG and GO enrichment analyses using the identified genes. The results of the KEGG analysis indicated that NAT10-related genes were enriched in pathways such as "ribosome biogenesis in eukaryotes", "spliceosome", "RNA transport", and the "mRNA surveillance pathway", among others (Fig. 8c). GO enrichment analysis showed that NAT10-related

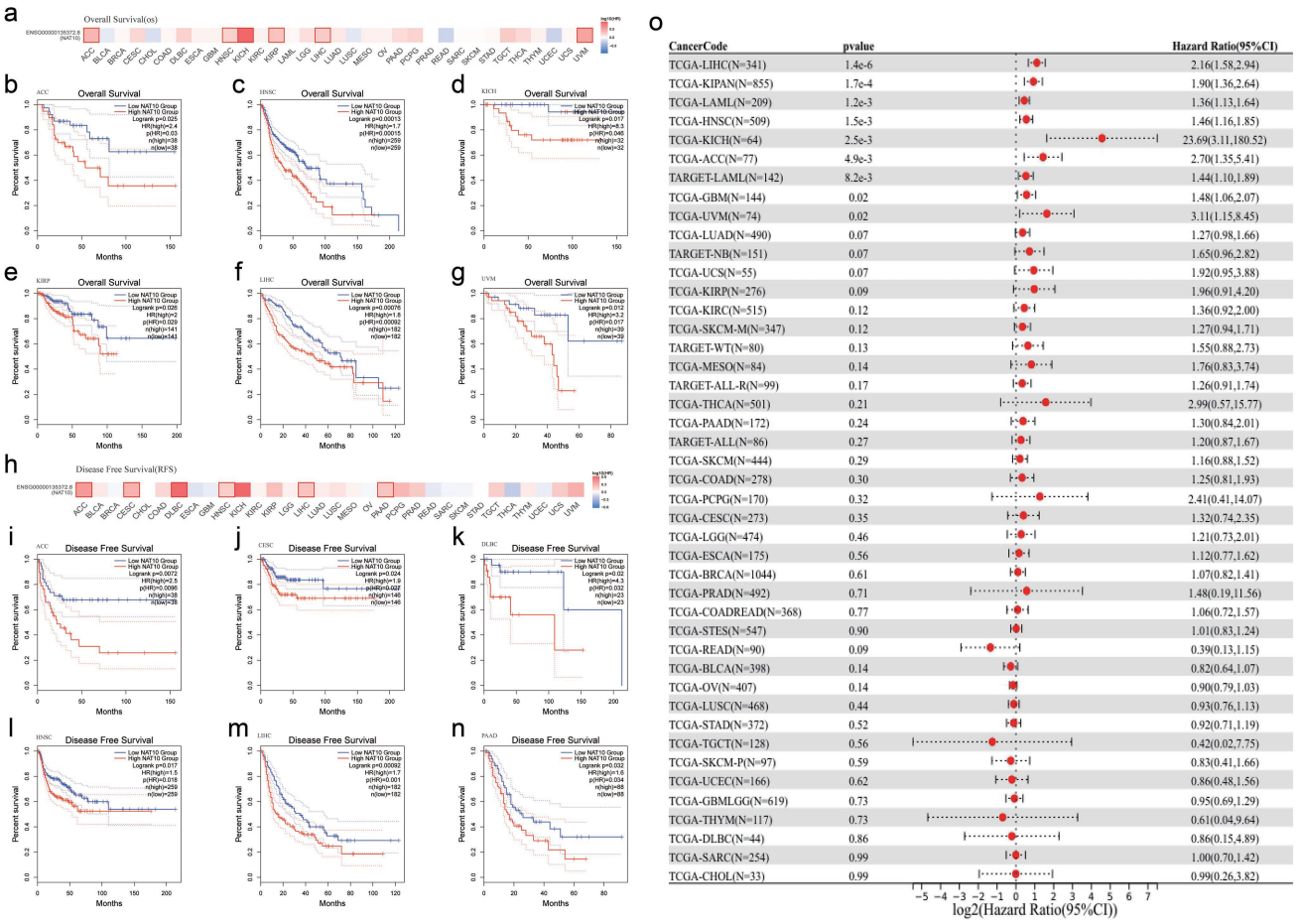


Fig. 5. Association between *NAT10* expression and survival outcomes across cancer types. (a) Overall survival significance map of NAT10 across TCGA cancer types. (b–g) Kaplan–Meier overall survival curves for ACC, HNSC, KICH, KIRP, LIHC, and UVM. (h) Disease-free survival significance map of NAT10 across TCGA cancer types. (i–n) Kaplan–Meier disease-free survival curves for ACC, CESC, DLBC, HNSC, LIHC, and PAAD. (o) Forest plot showing hazard ratios (HRs) and 95% confidence intervals (CIs) for the association between *NAT10* expression and overall survival across available pan-cancer cohorts in the UCSC Xena dataset. ACC, adrenocortical carcinoma; ALL, acute lymphoblastic leukemia; BLCA, bladder urothelial carcinoma; BRCA, breast invasive carcinoma; CESC, cervical squamous cell carcinoma and endocervical adenocarcinoma; CHOL, cholangiocarcinoma; COAD, colon adenocarcinoma; COADREAD, combined colon and rectum adenocarcinoma cohort; DLBC, diffuse large B-cell lymphoma; ESCA, esophageal carcinoma; GBM, glioblastoma multiforme; GBMLGG, combined glioblastoma and lower-grade glioma cohort; HNSC, head and neck squamous cell carcinoma; KICH, kidney chromophobe; KIPAN, pan-kidney cohort; KIRC, kidney renal clear cell carcinoma; KIRP, kidney renal papillary cell carcinoma; LAML, acute myeloid leukemia; LGG, brain lower-grade glioma; LIHC, liver hepatocellular carcinoma; LUAD, lung adenocarcinoma; LUSC, lung squamous cell carcinoma; MESO, mesothelioma; NAT10, N-acetyltransferase 10; NB, neuroblastoma; OV, ovarian serous cystadenocarcinoma; PAAD, pancreatic adenocarcinoma; PCPG, pheochromocytoma and paraganglioma; PRAD, prostate adenocarcinoma; READ, rectum adenocarcinoma; SARC, sarcoma; SKCM, skin cutaneous melanoma; SKCM-M, metastatic skin cutaneous melanoma; SKCM-P, primary skin cutaneous melanoma; STAD, stomach adenocarcinoma; STES, combined stomach and esophageal carcinoma cohort; TARGET, Therapeutically Applicable Research to Generate Effective Treatments; TCGA, The Cancer Genome Atlas; TGCT, testicular germ cell tumors; THCA, thyroid carcinoma; THYM, thymoma; UCEC, uterine corpus endometrial carcinoma; UCS, uterine carcinosarcoma; UCSC, University of California, Santa Cruz; UVM, uveal melanoma; WT, Wilms tumor.

genes were associated with terms including RNA binding, nucleolus, and nucleoplasm, among others (Fig. 8d). These enrichment results indicate functional associations of NAT10-related genes and interacting proteins and should not be interpreted as evidence of direct regulation of these pathways by NAT10.

Characteristics of NAT10 mutations in the TCGA pan-cancer cohort

To characterize NAT10-related genomic and molecular features across cancers, we analyzed *NAT10* alteration frequency, mutation sites and types, tumor mutational burden, and associations with RNA-modification-related genes. We found that 30 cancer types

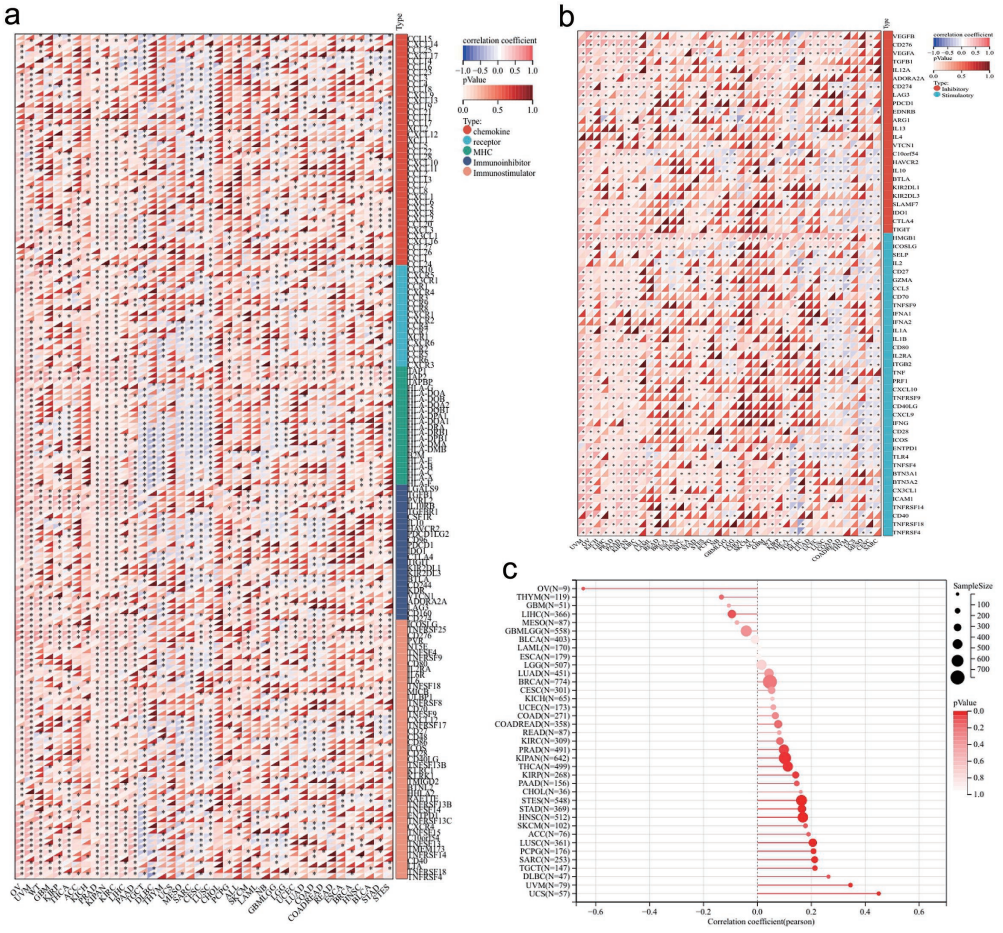


Fig. 6. Associations between *NAT10* expression and immune-related molecular features. (a) Pan-cancer correlations between *NAT10* expression and immune-regulatory genes, including chemokines, receptors, MHC-related genes, immunoinhibitors, and immunostimulators. (b) Pan-cancer correlations between *NAT10* expression and immune-checkpoint-related genes. (c) Pearson correlations between *NAT10* expression and the DNA methylation-based stemness score (DNAss) across cancer types. ACC, adrenocortical carcinoma; BLCA, bladder urothelial carcinoma; BRCA, breast invasive carcinoma; CESC, cervical squamous cell carcinoma and endocervical adenocarcinoma; CHOL, cholangiocarcinoma; COAD, colon adenocarcinoma; COADREAD, combined colon and rectum adenocarcinoma cohort; DLBC, diffuse large B-cell lymphoma; ESCA, esophageal carcinoma; GBM, glioblastoma multiforme; GBMLGG, combined glioblastoma and lower-grade glioma cohort; HNSC, head and neck squamous cell carcinoma; KICH, kidney chromophobe; KIPAN, pan-kidney cohort; KIRC, kidney renal clear cell carcinoma; KIRP, kidney renal papillary cell carcinoma; LAML, acute myeloid leukemia; LGG, brain lower-grade glioma; LIHC, liver hepatocellular carcinoma; LUAD, lung adenocarcinoma; LUSC, lung squamous cell carcinoma; MESO, mesothelioma; MHC, major histocompatibility complex; NAT10, N-acetyltransferase 10; OV, ovarian serous cystadenocarcinoma; PAAD, pancreatic adenocarcinoma; PCPG, pheochromocytoma and paraganglioma; PRAD, prostate adenocarcinoma; READ, rectum adenocarcinoma; SARC, sarcoma; SKCM, skin cutaneous melanoma; STAD, stomach adenocarcinoma; STES, combined stomach and esophageal carcinoma cohort; TGCT, testicular germ cell tumors; THCA, thyroid carcinoma; THYM, thymoma; UCEC, uterine corpus endometrial carcinoma; UCS, uterine carcinosarcoma; UVM, uveal melanoma.

exhibited *NAT10* alterations, with uterine corpus endometrial carcinoma having the highest alteration frequency of 6.4% (Fig. 9a). The analysis characterized the types, locations, and numbers of cases with *NAT10* mutations. Missense mutations were the predominant *NAT10* mutation type (Fig. 9b). To better understand the role of NAT10 in tumors, we examined the relationship between genomic heterogeneity and *NAT10* gene expression. We analyzed the association between TMB and *NAT10* expression across 37 tumor types. At the nominal *P*-value threshold, *NAT10* expression was positively correlated with TMB in stomach adenocarcinoma (STAD) and negatively correlated with TMB in colon adenocarcinoma (COAD), thyroid carcinoma (THCA), and cholangiocarcinoma (CHOL) (Fig. 9c). To further characterize the associations between NAT10 and RNA-modification-related genes, we analyzed the correlations between *NAT10* expression and 44 RNA-modification-related genes, comprising 10 m1A-related, 13 m5C-related, and 21 m6A-related genes (Fig. 9d). Collectively, these findings demonstrate cancer-type heterogeneity in the genomic alterations of NAT10 and its associations with tumor mutational burden and RNA-modification-related genes.

 DOI: 10.14218/CSP.2026.00017 | 2026

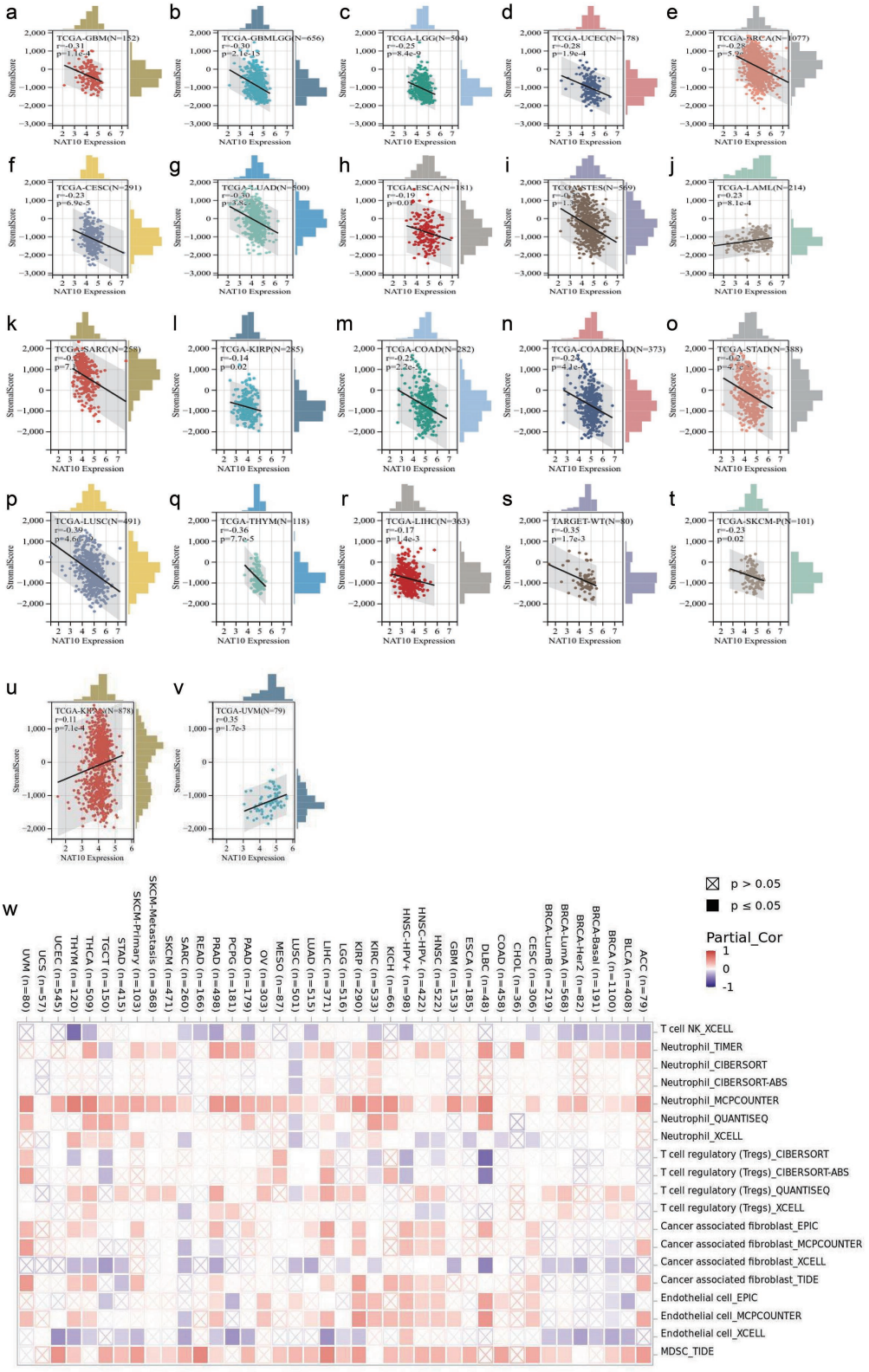


Fig. 7. Associations between *NAT10* expression and tumor microenvironment-related features across cancer types. (a–v) Correlations between *NAT10*

expression and ESTIMATE-derived stromal scores across the indicated cancer cohorts. Pearson correlation coefficients and corresponding *P* values are shown in each panel. (w) Pan-cancer associations between *NAT10* expression and estimated infiltration levels of selected immune and stromal cell populations assessed using multiple TIMER2.0 algorithms, including xCell, TIMER, CIBERSORT, CIBERSORT-ABS, QUANTISEQ, MCP-counter, EPIC, and TIDE. Colors indicate correlation coefficients, and crossed cells indicate statistically nonsignificant associations. ACC, adrenocortical carcinoma; BLCA, bladder urothelial carcinoma; BRCA, breast invasive carcinoma; CESC, cervical squamous cell carcinoma and endocervical adenocarcinoma; CHOL, cholangiocarcinoma; CIBERSORT, Cell-type Identification By Estimating Relative Subsets Of RNA Transcripts; CIBERSORT-ABS, CIBERSORT absolute mode; COAD, colon adenocarcinoma; COADREAD, combined colon and rectum adenocarcinoma cohort; DLBC, diffuse large B-cell lymphoma; EPIC, Estimating the Proportions of Immune and Cancer cells; ESCA, esophageal carcinoma; GBM, glioblastoma multiforme; GBMLGG, combined glioblastoma and lower-grade glioma cohort; HER2, human epidermal growth factor receptor 2; HNSC, head and neck squamous cell carcinoma; HPV, human papillomavirus; KICH, kidney chromophobe; KIPAN, pan-kidney cohort; KIRC, kidney renal clear cell carcinoma; KIRP, kidney renal papillary cell carcinoma; LAML, acute myeloid leukemia; LGG, brain lower-grade glioma; LIHC, liver hepatocellular carcinoma; LUAD, lung adenocarcinoma; LumA, luminal A; LumB, luminal B; LUSC, lung squamous cell carcinoma; MCP-counter, Microenvironment Cell Populations-counter; MDSC, myeloid-derived suppressor cell; MESO, mesothelioma; NAT10, N-acetyltransferase 10; NK, natural killer; OV, ovarian serous cystadenocarcinoma; PAAD, pancreatic adenocarcinoma; Partial_Cor, partial correlation coefficient; PCPG, pheochromocytoma and paraganglioma; PRAD, prostate adenocarcinoma; QUANTISEQ, quanTIseq immune-cell deconvolution algorithm; READ, rectum adenocarcinoma; SARC, sarcoma; SKCM, skin cutaneous melanoma; SKCM-P, primary skin cutaneous melanoma; STAD, stomach adenocarcinoma; STES, combined stomach and esophageal carcinoma cohort; TARGET, Therapeutically Applicable Research to Generate Effective Treatments; TCGA, The Cancer Genome Atlas; TGCT, testicular germ cell tumors; THCA, thyroid carcinoma; THYM, thymoma; TIDE, Tumor Immune Dysfunction and Exclusion; TIMER, Tumor Immune Estimation Resource; TIMER2.0, Tumor Immune Estimation Resource 2.0; Tregs, regulatory T cells; UCEC, uterine corpus endometrial carcinoma; UCS, uterine carcinosarcoma; UVM, uveal melanoma; WT, Wilms tumor; xCell, xCell cell-type enrichment algorithm.

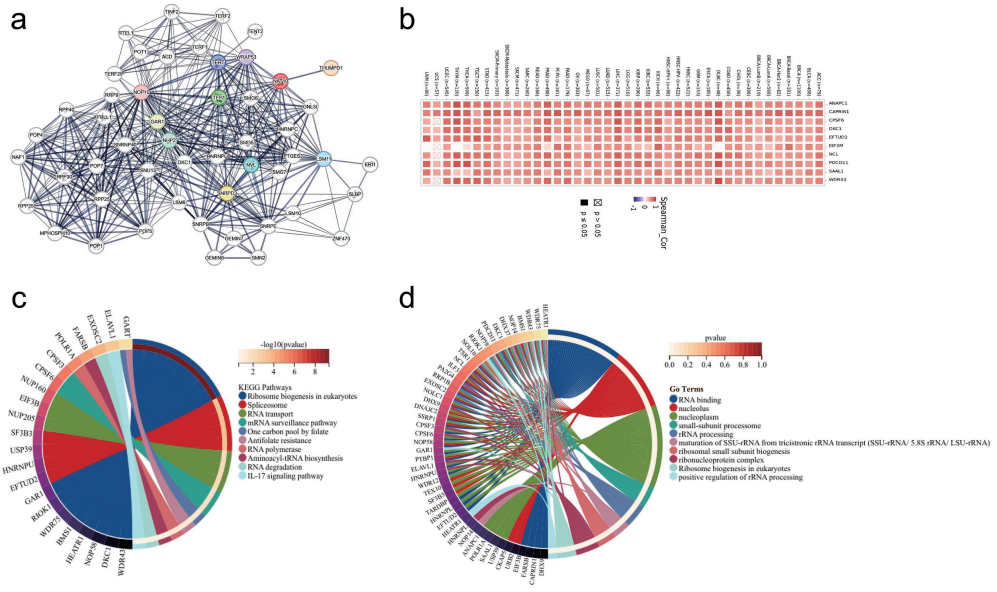


Fig. 8. NAT10-related protein interaction, gene-correlation, and enrichment analyses. (a) Protein–protein interaction network of experimentally supported NAT10-interacting proteins obtained from STRING. (b) Pan-cancer Spearman correlations between *NAT10* expression and the top 10 NAT10-associated genes identified using GEPIA2. (c) KEGG pathway enrichment analysis of NAT10-interacting and correlated genes. (d) Gene Ontology enrichment analysis of NAT10-interacting and correlated genes. ACC, adrenocortical carcinoma; BLCA, bladder urothelial carcinoma; BRCA, breast invasive carcinoma; CESC, cervical squamous cell carcinoma and endocervical adenocarcinoma; CHOL, cholangiocarcinoma; COAD, colon adenocarcinoma; DLBC, diffuse large B-cell lymphoma; ESCA, esophageal carcinoma; GBM, glioblastoma multiforme; GEPIA2, Gene Expression Profiling Interactive Analysis 2; GO, Gene Ontology; HER2, human epidermal growth factor receptor 2; HNSC, head and neck squamous cell carcinoma; HPV, human papillomavirus; IL-17, interleukin-17; KEGG, Kyoto Encyclopedia of Genes and Genomes; KICH, kidney chromophobe; KIRC, kidney renal clear cell carcinoma; KIRP, kidney renal papillary cell carcinoma; LGG, brain lower-grade glioma; LIHC, liver hepatocellular carcinoma; LUAD, lung adenocarcinoma; LumA, luminal A; LumB, luminal B; LSU, large subunit; LUSC, lung squamous cell carcinoma; MESO, mesothelioma; mRNA, messenger RNA; NAT10, N-acetyltransferase 10; OV, ovarian serous cystadenocarcinoma; PAAD, pancreatic adenocarcinoma; PCPG, pheochromocytoma and paraganglioma; PRAD, prostate adenocarcinoma; READ, rectum adenocarcinoma; rRNA, ribosomal RNA; SARC, sarcoma; SKCM, skin cutaneous melanoma; SSU, small subunit; STAD, stomach adenocarcinoma; STRING, Search Tool for the Retrieval of Interacting Genes/Proteins; TGCT, testicular germ cell tumors; THCA, thyroid carcinoma; THYM, thymoma; tRNA, transfer RNA; UCEC, uterine corpus endometrial carcinoma; UCS, uterine carcinosarcoma; UVM, uveal melanoma.

 DOI: 10.14218/CSP.2026.00017 | 2026

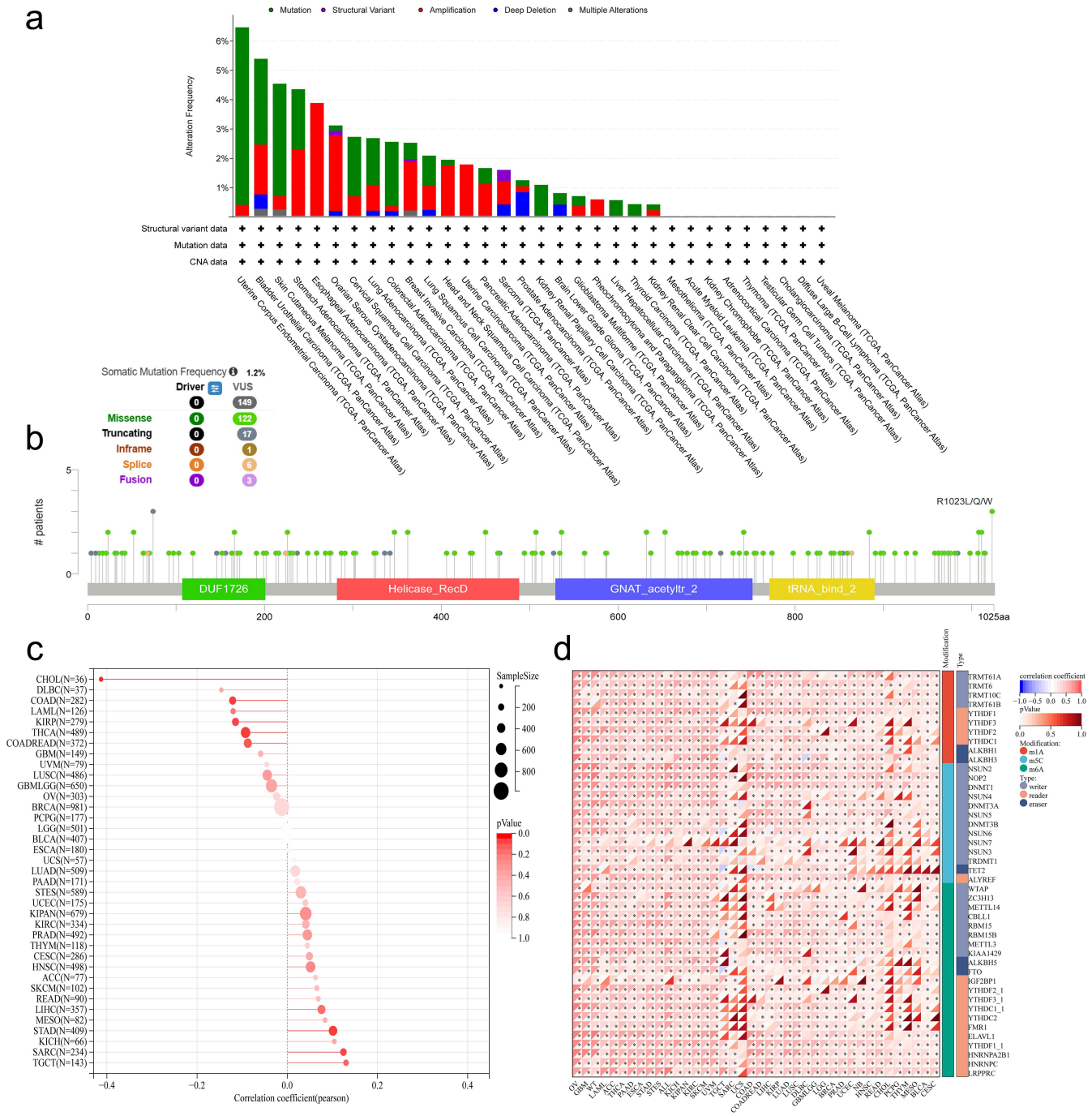


Fig. 9. Genomic alterations of NAT10 and associated molecular features across cancers. (a) Frequency and distribution of *NAT10* genomic alterations across cancer types analyzed using cBioPortal, including mutations, structural variants, amplifications, deep deletions, and multiple alterations. (b) Distribution of *NAT10* somatic mutations across the NAT10 protein sequence, showing mutation types, mutation locations, numbers of affected cases, and annotated protein domains. (c) Pearson correlations between *NAT10* expression and TMB across cancer types; dot size represents sample size and color represents the corresponding nominal *P* value. (d) Pan-cancer correlation heatmap between *NAT10* expression and 44 RNA-modification-related genes, comprising m1A-, m5C-, and m6A-related regulators. Correlation coefficients and corresponding *P* values are shown in the heatmap, and side annotations indicate the RNA-modification category and functional class of each regulator. aa, amino acids; ACC, adrenocortical carcinoma; BLCA, bladder urothelial carcinoma; BRCA, breast invasive carcinoma; CESC, cervical squamous cell carcinoma and endocervical adenocarcinoma; CHOL, cholangiocarcinoma; CNA, copy number alteration; COAD, colon adenocarcinoma; COADREAD, combined colon and rectum adenocarcinoma cohort; DLBC, diffuse large B-cell

lymphoma; DUF1726, domain of unknown function 1726; ESCA, esophageal carcinoma; GBM, glioblastoma multiforme; GBMLGG, combined glioblastoma and lower-grade glioma cohort; GNAT, Gcn5-related N-acetyltransferase; KICH, kidney chromophobe; KIPAN, pan-kidney cohort; KIRC, kidney renal clear cell carcinoma; KIRP, kidney renal papillary cell carcinoma; LAML, acute myeloid leukemia; LGG, brain lower-grade glioma; LIHC, liver hepatocellular carcinoma; LUAD, lung adenocarcinoma; LUSC, lung squamous cell carcinoma; m1A, N1-methyladenosine; m5C, 5-methylcytosine; m6A, N6-methyladenosine; MESO, mesothelioma; NAT10, N-acetyltransferase 10; OV, ovarian serous cystadenocarcinoma; PAAD, pancreatic adenocarcinoma; PCPG, pheochromocytoma and paraganglioma; PRAD, prostate adenocarcinoma; READ, rectum adenocarcinoma; RecD, recombination protein D; SARC, sarcoma; SKCM, skin cutaneous melanoma; STAD, stomach adenocarcinoma; STES, combined stomach and esophageal carcinoma cohort; TCGA, The Cancer Genome Atlas; TGCT, testicular germ cell tumors; THCA, thyroid carcinoma; THYM, thymoma; TMB, tumor mutational burden; tRNA, transfer RNA; UCEC, uterine corpus endometrial carcinoma; UCS, uterine carcinosarcoma; UVM, uveal melanoma; VUS, variant of uncertain significance.

Functional enrichment analysis of NAT10 in BRCA and ESCA

We further examined the cancer-specific molecular and functional characteristics of NAT10 in BRCA. The mutation profile showed the types, locations, and numbers of *NAT10* mutation cases in BRCA, with missense mutations representing the predominant mutation type (Fig. 1a). Representative HPA immunohistochemical images were used to visualize NAT10 protein staining in breast cancer tissues (Fig. 1b–c). The top 50 genes positively and negatively correlated with *NAT10* expression in BRCA are shown in Fig. 1d–e. Gene set enrichment analysis identified pathways including RNA transport, pyrimidine metabolism, and ribosome biogenesis in eukaryotes (Fig. 1f). GO biological-process analysis further showed enrichment of processes including non-coding RNA (ncRNA) processing, RNA modification, and tRNA metabolic processes (Fig. 1g).

We additionally selected ESCA for cancer-specific exploration because NAT10 was significantly upregulated in ESCA in our pan-cancer expression analysis and complementary functional data were available for further characterization. *NAT10* mutations in ESCA were characterized by type, location, and frequency. In ESCA, missense mutations were the predominant *NAT10* mutation type, as shown in Fig. 2a. Representative HPA immunofluorescence imaging showed predominantly nucleolar localization of NAT10 at the cellular level (Fig. 2b). This image was used to illustrate the subcellular localization of NAT10 rather than cancer-type-specific protein expression. KEGG analysis revealed an enrichment of pathways related to Ribosome biogenesis in eukaryotes, RNA transport, and aminoacyl-tRNA biosynthesis, among others (Fig. 2c). The GO analysis of biological processes demonstrated that NAT10 was mainly associated with functions such as DNA replication, double-strand break repair, and cell cycle checkpoint (Fig. 2d). Subsequently, the correlation between NAT10 and 14 cancer functional states was analyzed using single-cell sequencing data from CancerSEA (Fig. 2e). For ESCA, a significant positive correlation was observed between *NAT10* expression and angiogenesis, differentiation, and inflammation. Conversely, a negative correlation was found between *NAT10* expression and cell cycle, DNA damage, and DNA repair (Fig. 2f). These findings further characterize the molecular and functional associations of NAT10 in ESCA.

Association between NAT10 expression and survival outcomes following immune checkpoint blockade

To explore the association between *NAT10* expression and survival outcomes according to ICB treatment, we analyzed overall survival in patients stratified by *NAT10* expression. In patients who did not receive immunotherapy, *NAT10* expression was not significantly associated with overall survival (HR = 1.10, 95% CI: 0.93–1.30, $P = 0.26$; Fig. 10a). Higher *NAT10* expression was nominally associated with longer overall survival in patients receiving any anti-PD-1 therapy (HR = 0.68, 95% CI: 0.52–0.90, $P = 0.0056$; Fig. 10b) and in the pembrolizumab-only group (HR = 0.47, 95% CI: 0.31–0.70, $P = 0.00019$; Fig. 10d), whereas no significant association was observed in the nivolumab-only group (HR = 1.21, 95% CI: 0.75–1.94, $P = 0.43$; Fig. 10c). Similarly, higher *NAT10* expression was nominally associated with longer overall survival in patients receiving any anti-PD-L1 therapy (HR = 0.72, 95% CI: 0.56–0.92, $P = 0.0079$; Fig. 10e) and in the atezolizumab-only group (HR = 0.73, 95% CI: 0.57–0.94, $P = 0.013$; Fig. 10f). No significant association was observed in patients receiving any anti-CTLA-4 therapy (HR = 0.66, 95% CI: 0.39–1.11, $P = 0.11$; Fig. 10g) or ipilimumab alone (HR = 0.66, 95% CI: 0.39–1.11, $P = 0.11$; Fig. 10h). Collectively, *NAT10* expression showed heterogeneous associations with overall survival across different ICB treatment groups. Given the exploratory nature and heterogeneity of these publicly available immunotherapy cohorts, these findings should not be interpreted as establishing NAT10 as a clinically validated predictive biomarker for immunotherapy response.

Discussion

In this retrospective pan-cancer analysis, we identified substantial cancer-type heterogeneity in the associations of NAT10 with tumor expression, pathological stage, survival, genomic alterations, RNA-related molecular programs, and immune characteristics. Three findings are particularly noteworthy. First, elevated *NAT10* expression was associated with adverse clinicopathological or survival features in selected, but not all, cancer types. Second, *NAT10* expression showed reproducible associations with multiple components of the tumor immune microenvironment, including positive associations with myeloid-derived suppressor cell and cancer-associated fibroblast infiltration estimates and negative associations with several T-cell and NK-cell populations.[14,31] Third, exploratory analyses of publicly available ICB cohorts revealed heterogeneous survival associations across treatment categories.[32] Together, these observations support a cancer-type-dependent rather than universally oncogenic interpretation of NAT10.

To elucidate the role of NAT10 in pan-cancer, we examined its expression in a variety of normal and tumor tissues in humans. We found that NAT10 is expressed in a range of tissues, suggesting its potential involvement in diverse physiological and pathological processes. NAT10 was more highly expressed in multiple tumor

 DOI: 10.14218/CSP.2026.00017 | 2026

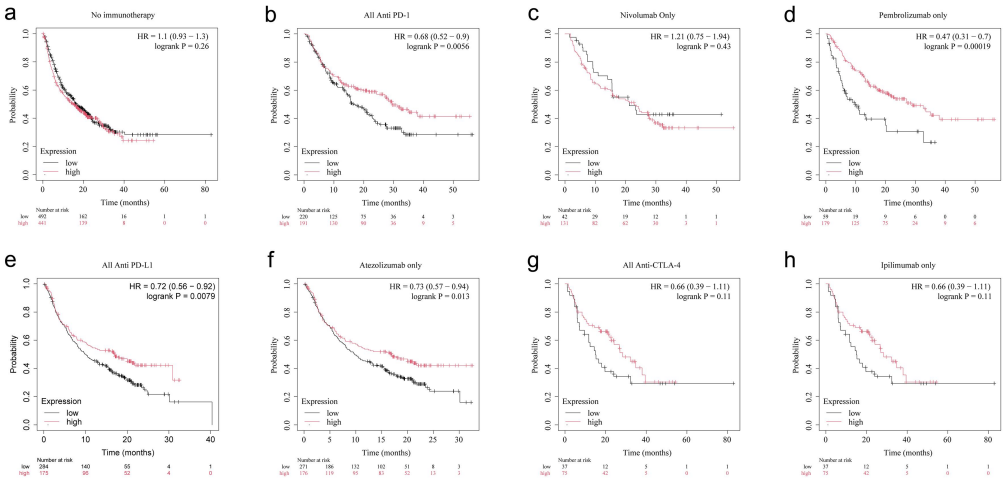


Fig. 10. Association between *NAT10* expression and overall survival in immune-checkpoint-blockade cohorts. Kaplan–Meier overall survival analyses according to *NAT10* expression in patients who did not receive immunotherapy (a), patients receiving any anti-PD-1 therapy (b), nivolumab alone (c), pembrolizumab alone (d), any anti-PD-L1 therapy (e), atezolizumab alone (f), any anti-CTLA-4 therapy (g), and ipilimumab alone (h). Hazard ratios, 95% confidence intervals, nominal log-rank *P* values, and numbers at risk are shown in the corresponding panels. CI, confidence interval; CTLA-4, cytotoxic T-lymphocyte-associated protein 4; HR, hazard ratio; NAT10, N-acetyltransferase 10; PD-1, programmed cell death protein 1; PD-L1, programmed death-ligand 1.

types than in corresponding non-tumor tissues, supporting a possible association with tumor-related biological processes.[33] To further explore the significance of *NAT10* expression in cancer, we analyzed the correlation between *NAT10* expression and clinical stage and prognostic value. Stage-associated differences in *NAT10* expression were observed in selected cancer types. In some cancers, high *NAT10* expression showed significant prognostic associations, although these associations varied substantially among tumor types. Our survival analyses further showed that higher *NAT10* expression was associated with poorer overall and disease-free survival in selected tumor types. These findings suggest that NAT10 may have potential prognostic relevance in selected cancer types.[4,7] However, further independent validation is required before NAT10 can be considered for clinical prognostic or therapeutic applications. The cancer-type-specific prognostic heterogeneity may reflect differences in the biological programs through which NAT10 is involved in different tumor contexts. For example, previous cancer-specific studies have linked NAT10 to ferroptosis suppression in colorectal cancer, DNA-repair-associated chemoresistance in bladder cancer, immune regulation, and metastatic progression in ESCA.[5,6,13,14] These observations suggest that the clinical consequences of *NAT10* expression may depend on the relative contribution of RNA-processing, stress-response, DNA-repair, metabolic, and immune programs in individual malignancies. However, the present pan-cancer analyses are correlative and cannot determine which mechanism predominates in a given cancer type.

A prominent finding of our immune analyses was the association of higher *NAT10* expression with increased estimated infiltration of myeloid-derived suppressor cells and cancer-associated fibroblasts, together with lower estimated infiltration of several T-cell and NK-cell populations.[14] This pattern is compatible with an immunosuppressive or immune-excluded microenvironment in some tumor contexts.[34-36] Importantly, however, the direction and magnitude of these associations varied across cancer types, and computational deconvolution cannot determine whether NAT10 directly regulates immune-cell recruitment or instead reflects broader tumor-intrinsic transcriptional states.[18,37]

The genomic analyses further demonstrated that *NAT10* alterations were generally infrequent and heterogeneous across tumor types, with UCEC showing the highest alteration frequency in the analyzed cohorts. In parallel, *NAT10* expression was associated with TMB only in a limited number of tumor types.[38] These results suggest that NAT10-related biology is unlikely to be explained by recurrent genomic alteration alone and may instead be more closely related to transcriptional and post-transcriptional regulation. Consistent with this interpretation, NAT10-associated genes were predominantly enriched in RNA-processing, ribosome-biogenesis, RNA-transport, and related pathways.[10]

These enrichment and co-expression findings provide additional molecular context for NAT10-associated biology but do not establish direct mechanistic regulation. To explore the potential treatment-associated relevance of NAT10, we examined the relationship between *NAT10* expression and overall survival across publicly available ICB-treated cohorts. In patients who did not receive immunotherapy, *NAT10* expression was not significantly associated with overall survival. Interestingly, higher *NAT10* expression was associated with longer overall survival in the pooled anti-PD-1 group, the pembrolizumab-only subgroup, the pooled anti-PD-L1 group, and the atezolizumab-only subgroup, whereas no statistically significant association was observed in the nivolumab-only, pooled anti-CTLA-4, or ipilimumab-only groups. Although both nivolumab and pembrolizumab target the PD-1 pathway, the association between *NAT10* expression and overall survival differed between the corresponding treatment subgroups. Such heterogeneity may reflect differences in cancer type, treatment indication, cohort composition, and other unmeasured clinical or molecular factors.[39] At first glance, this observation appears

to contrast with the immune-infiltration pattern described above. However, a prognostic association within an ICB-treated cohort is not equivalent to evidence that NAT10 promotes antitumor immunity or predicts treatment response.[16] Tumors with high *NAT10* expression may simultaneously exhibit immunosuppressive features and retain molecular characteristics associated with sensitivity to PD-1/PD-L1 blockade, while differences in tumor type, treatment indication, baseline immune activity, PD-L1 expression, mutational burden, and prior therapy may further modify this relationship.[15] Because these variables could not be uniformly adjusted across the pooled public cohorts, the present analysis cannot distinguish a treatment-predictive effect from prognostic or confounding effects. Therefore, these findings should be considered exploratory and require validation in cancer-specific and independently annotated immunotherapy cohorts.

Overall, this study highlights cancer-type-dependent associations of NAT10 with prognosis, genomic features, and the tumor immune microenvironment. However, the biological mechanisms underlying these associations and their clinical relevance remain to be established in experimental models, independent cohorts, and prospective studies. The current study provides primarily association-based evidence because it relies on publicly available datasets and lacks independent experimental validation. Future studies using cancer-specific cellular and animal models, together with independent clinical cohorts, will be required to determine whether the associations identified here reflect functionally relevant NAT10-dependent mechanisms and whether NAT10 has sufficient robustness for biomarker development.[40]

Limitations

Several limitations should be considered when interpreting this study. First, the analyses were retrospective and based predominantly on publicly available datasets; therefore, the observed associations cannot establish causality. Second, differences in sample processing, sequencing platforms, normalization strategies, and cohort composition across TCGA, GTEx, and other databases may introduce batch effects and inter-database heterogeneity.[41] Third, several analyses were performed across cancer types with markedly different sample sizes, and findings from relatively small cohorts may be statistically unstable. Fourth, the pan-cancer survival analyses were primarily univariable and did not uniformly adjust for age, stage, treatment, molecular subtype, or other clinicopathological confounders. Fifth, the immunotherapy analyses integrated heterogeneous public cohorts and lacked harmonized individual-level information on cancer type, treatment line, PD-L1 status, TMB, and other relevant covariates; consequently, these results should be regarded as hypothesis-generating rather than evidence of predictive clinical utility. Sixth, HPA images were used for qualitative visualization and were not quantitatively analyzed. Finally, no independent clinical cohort or experimental validation was included. Prospective cohorts and mechanistic experiments will therefore be required to validate the biological and clinical relevance of NAT10 in specific cancer contexts.

Conclusions

In summary, this retrospective multi-database pan-cancer analysis demonstrates that the expression, prognostic relevance, genomic characteristics, and immune associations of NAT10 vary substantially across cancer types. Elevated *NAT10* expression is associated with adverse clinicopathological or survival features in selected malignancies and with distinct patterns of immune-cell infiltration. Exploratory ICB analyses further identify treatment-group-dependent survival associations, but these findings do not establish NAT10 as a predictive biomarker for immunotherapy. Overall, our results support further cancer-specific investigation of NAT10 and provide a framework for subsequent validation in independent clinical cohorts and mechanistic studies.

Supporting information

Supplementary material for this article is available at https://doi.org/10.14218/CSP.2026.00017.

Acknowledgments

None.

Funding

This study was supported by grants from the National Natural Science Foundation of China (82404088); Jiangsu Provincial Basic Research Special Fund (Natural Science Foundation) Youth Fund (BK20241683); Postgraduate Research & Practice Innovation Program of Jiangsu Province (26CXJH0707).

Conflict of interest

One of the authors, Prof. Ruihua Shi has served as an executive associate editor of *Cancer Screening and Prevention* since February 2022. All other authors have no conflicts of interest related to this manuscript.

Author contributions

Conceptualization (YD, RS), data collection and analysis (YD), bioinformatics analysis (YD), methodology (LR), visualization (YD), supervision (LR, RS), resources (RS), funding acquisition (RS), writing—original draft (YD), and writing—review and editing (LR, RS). All authors read and approved the final version of the manuscript.

Ethical statement

This study is entirely based on de-identified public databases; no research ethics committee approval was required, and this work complies with the principles of the Declaration of Helsinki, as revised in 2024.

Data sharing statement

The present study was entirely based on publicly available, de-identified datasets and web-based analytical platforms, including TCGA, GTEx, HPA, UCSC Xena, GEPIA2, cBioPortal, TIMER2.0, STRING, LinkedOmics, CancerSEA, and Kaplan–Meier Plotter. The corresponding access routes are provided in the Materials and Methods section. No new raw data were generated in this study. Processed data underlying the figures are available

from the corresponding author upon reasonable request. Analytical workflows were based on publicly accessible platform settings together with standard statistical analyses performed in R.

References

[1] Arango D, Sturgill D, Alhusaini N, Dillman AA, Sweet TJ, Hanson G, *et al*. Acetylation of Cytidine in mRNA Promotes Translation Efficiency. Cell 2018;175(7):1872–1886.e24. DOI: 10.1016/j.cell.2018.10.030, PMID: 30449621.

[2] Wiener D, Schwartz S. The epitranscriptome beyond m(6)A. Nat Rev Genet 2021;22(2):119–131. DOI: 10.1038/s41576-020-00295-8, PMID: 33188361.

[3] Roundtree IA, Evans ME, Pan T, He C. Dynamic RNA Modifications in Gene Expression Regulation. Cell 2017;169(7):1187–1200. DOI: 10.1016/j.cell.2017.05.045, PMID: 28622506.

[4] Han Y, Zhang X, Miao L, Lin H, Zhuo Z, He J, *et al*. Biological function and mechanism of NAT10 in cancer. Cancer Innov 2025;4(1):e154. DOI: 10.1002/cai2.154, PMID: 39817252.

[5] Zheng X, Wang Q, Zhou Y, Zhang D, Geng Y, Hu W, *et al*. N-acetyltransferase 10 promotes colon cancer progression by inhibiting ferroptosis through N4-acetylation and stabilization of ferroptosis suppressor protein 1 (FSP1) mRNA. Cancer Commun (Lond) 2022;42(12):1347–1366. DOI: 10.1002/cac2.12363, PMID: 36209353.

[6] Xie R, Cheng L, Huang M, Huang L, Chen Z, Zhang Q, *et al*. NAT10 Drives Cisplatin Chemoresistance by Enhancing ac4C-Associated DNA Repair in Bladder Cancer. Cancer Res 2023;83(10):1666–1683. DOI: 10.1158/0008-5472.CAN-22-2233, PMID: 36939377.

[7] Yang C, Wu T, Zhang J, Liu J, Zhao K, Sun W, *et al*. Prognostic and Immunological Role of mRNA ac4C Regulator NAT10 in Pan-Cancer: New Territory for Cancer Research? Front Oncol 2021;11:630417. DOI: 10.3389/fonc.2021.630417, PMID: 34094911.

[8] Wang L, Tao Y, Zhai J, Xue M, Zheng C, Hu H. The emerging roles of ac4C acetylation "writer" NAT10 in tumorigenesis: A comprehensive review. Int J Biol Macromol 2024;254(Pt 2):127789. DOI: 10.1016/j.ijbiomac.2023.127789, PMID: 37926318.

[9] Achour C, Oberdoerffer S. NAT10 and cytidine acetylation in mRNA: intersecting paths in development and disease. Curr Opin Genet Dev 2024;87:102207. DOI: 10.1016/j.gde.2024.102207, PMID: 38820741.

[10] Ito S, Horikawa S, Suzuki T, Kawauchi H, Tanaka Y, Suzuki T, *et al*. Human NAT10 is an ATP-dependent RNA acetyltransferase responsible for N4-acetylcytidine formation in 18 S ribosomal RNA (rRNA). J Biol Chem 2014;289(52):35724–35730. DOI: 10.1074/jbc.C114.602698, PMID: 25411247.

[11] An Y, Duan H. The role of m6A RNA methylation in cancer metabolism. Mol Cancer 2022;21(1):14. DOI: 10.1186/s12943-022-01500-4, PMID: 35022030.

[12] Zhang Y, Lei Y, Dong Y, Chen S, Sun S, Zhou F, *et al*. Emerging roles of RNA ac4C modification and NAT10 in mammalian development and human diseases. Pharmacol Ther 2024;253:108576. DOI: 10.1016/j.pharmthera.2023.108576, PMID: 38065232.

[13] Liu WC, Wei YH, Chen JF, Xing XL, Jia HX, Yang XY, *et al*. Inhibition of tumor-intrinsic NAT10 enhances antitumor immunity by triggering type I interferon response via MYC/CDK2/DNMT1 pathway. Nat Commun 2025;16(1):5154. DOI: 10.1038/s41467-025-60293-4, PMID: 40461504.

[14] Liu J, Gu Z, Zou L, Zhang Z, Shen L, Wang R, *et al*. Acetyltransferase NAT10 promotes an immunosuppressive microenvironment by modulating CD8(+) T cell activity in prostate cancer. Mol Biomed 2024;5(1):67. DOI: 10.1186/s43556-024-00228-5, PMID: 39648231.

[15] Havel JJ, Chowell D, Chan TA. The evolving landscape of biomarkers for checkpoint inhibitor immunotherapy. Nat Rev Cancer 2019;19(3):133–150. DOI: 10.1038/s41568-019-0116-x, PMID: 30755690.

[16] Ballman KV. Biomarker: Predictive or Prognostic? J Clin Oncol 2015;33(33):3968–3971. DOI: 10.1200/JCO.2015.63.3651, PMID: 26392104.

[17] Uhlén M, Fagerberg L, Hallström BM, Lindskog C, Oksvold P, Mardinoglu A, *et al*. Proteomics. Tissue-based map of the human proteome. Science 2015;347(6220):1260419. DOI: 10.1126/science.1260419, PMID: 25613900.

[18] Li T, Fu J, Zeng Z, Cohen D, Li J, Chen Q, *et al*. TIMER2.0 for analysis of tumor-infiltrating immune cells. Nucleic Acids Res 2020;48(W1):W509–W514. DOI: 10.1093/nar/gkaa407, PMID: 32442275.

[19] Weinstein JN, Collisson EA, Mills GB, Shaw KR, Ozenberger BA, Ellrott K, *et al*. The Cancer Genome Atlas Pan-Cancer analysis project. Nat Genet 2013;45(10):1113–1120. DOI: 10.1038/ng.2764, PMID: 24071849.

[20] GTEx Consortium. The GTEx Consortium atlas of genetic regulatory effects across human tissues. Science 2020;369(6509):1318–1330. DOI: 10.1126/science.aaz1776, PMID: 32913098.

[21] Tang Z, Kang B, Li C, Chen T, Zhang Z. GEPIA2: an enhanced web server for large-scale expression profiling and interactive analysis. Nucleic Acids Res 2019;47(W1):W556–W560. DOI: 10.1093/nar/gkz430, PMID: 31114875.

[22] Goldman MJ, Craft B, Hastie M, Repečka K, McDade F, Kamath A, *et al*. Visualizing and interpreting cancer genomics data via the Xena platform. Nat Biotechnol 2020;38(6):675–678. DOI: 10.1038/s41587-020-0546-8, PMID: 32444850.

[23] Yoshihara K, Shahmoradgoli M, Martínez E, Vegesna R, Kim H, Torres-Garcia W, *et al*. Inferring tumour purity and stromal and immune cell admixture from expression data. Nat Commun 2013;4:2612. DOI: 10.1038/ncomms3612, PMID: 24113773.

[24] Szklarczyk D, Kirsch R, Koutrouli M, Nastou K, Mehryary F, Hachilif R, *et al*. The STRING database in 2023: protein-protein association networks and functional enrichment analyses for any sequenced genome of interest. Nucleic Acids Res 2023;51(D1):D638–D646. DOI: 10.1093/nar/gkac1000, PMID: 36370105.

[25] Shen W, Song Z, Zhong X, Huang M, Shen D, Gao P, *et al*. Sangerbox: A comprehensive, interaction-friendly clinical bioinformatics analysis platform. iMeta 2022;1(3):e36. DOI: 10.1002/imt2.36, PMID: 38868713.

[26] Gao J, Aksoy BA, Dogrusoz U, Dresdner G, Gross B, Sumer SO, *et al*. Integrative analysis of complex cancer genomics and clinical profiles using the cBioPortal. Sci Signal 2013;6(269):pl1. DOI: 10.1126/scisignal.2004088, PMID: 23550210.

[27] Mayakonda A, Lin DC, Assenov Y, Plass C, Koeffler HP. Maftools: efficient and comprehensive analysis of somatic variants in cancer. Genome Res 2018;28(11):1747–1756. DOI: 10.1101/gr.239244.118, PMID: 30341162.

[28] Yuan H, Yan M, Zhang G, Liu W, Deng C, Liao G, *et al*. CancerSEA: a cancer single-cell state atlas. Nucleic Acids Res 2019;47(D1):D900–D908. DOI: 10.1093/nar/gky939, PMID: 30329142.

[29] Vasaikar SV, Straub P, Wang J, Zhang B. LinkedOmics: analyzing multi-omics data within and across 32 cancer types. Nucleic Acids Res 2018;46(D1):D956–D963. DOI: 10.1093/nar/gkx1090, PMID: 29136207.

[30] Kovács SA, Fekete JT, Győrffy B. Predictive biomarkers of immuno-

therapy response with pharmacological applications in solid tumors. Acta Pharmacol Sin 2023;44(9):1879–1889. DOI: 10.1038/s41401-023-01079-6, PMID: 37055532.

[31] Wang Z, Luo J, Huang H, Wang L, Lv T, Wang Z, *et al*. NAT10-mediated upregulation of GAS5 facilitates immune cell infiltration in non-small cell lung cancer via the MYBBP1A-p53/IRF1/type I interferon signaling axis. Cell Death Discov 2024;10(1):240. DOI: 10.1038/s41420-024-01997-2, PMID: 38762546.

[32] Chen DS, Mellman I. Elements of cancer immunity and the cancer-immune set point. Nature 2017;541(7637):321–330. DOI: 10.1038/nature21349, PMID: 28102259.

[33] Zhan YJ, Deng CM, Tang L, Li SJ, Xu TY, Wei X, *et al*. NAT10 Increases Lysosomal Acidification to Promote Esophageal Cancer Metastasis via ac4C Acetylation of ATP6V0E1 mRNA. Adv Sci (Weinh) 2025;12(31):e02931. DOI: 10.1002/advs.202502931, PMID: 40729677.

[34] Fridman WH, Pagès F, Sautès-Fridman C, Galon J. The immune contexture in human tumours: impact on clinical outcome. Nat Rev Cancer 2012;12(4):298–306. DOI: 10.1038/nrc3245, PMID: 22419253.

[35] Veglia F, Sanseviero E, Gabrilovich DI. Myeloid-derived suppressor cells in the era of increasing myeloid cell diversity. Nat Rev Immunol 2021;21(8):485–498. DOI: 10.1038/s41577-020-00490-y, PMID: 33526920.

[36] Sahai E, Astsaturov I, Cukierman E, DeNardo DG, Egeblad M, Evans RM, *et al*. A framework for advancing our understanding of cancer-associated fibroblasts. Nat Rev Cancer 2020;20(3):174–186. DOI: 10.1038/s41568-019-0238-1, PMID: 31980749.

[37] Sturm G, Finotello F, Petitprez F, Zhang JD, Baumbach J, Fridman WH, *et al*. Comprehensive evaluation of transcriptome-based cell-type quantification methods for immuno-oncology. Bioinformatics 2019;35(14):i436–i445. DOI: 10.1093/bioinformatics/btz363, PMID: 31510660.

[38] Samstein RM, Lee CH, Shoushtari AN, Hellmann MD, Shen R, Janjigian YY, *et al*. Tumor mutational load predicts survival after immunotherapy across multiple cancer types. Nat Genet 2019;51(2):202–206. DOI: 10.1038/s41588-018-0312-8, PMID: 30643254.

[39] Murphy JF. Personalized Vaccines: Unlocking the Next Era of Medical Innovation in Cancer Immunotherapy. Cancer Screen Prev 2025;4(4):199–204. DOI: 10.14218/CSP.2025.00023.

[40] Li Y, Bai Y, Yang M, Liu J, Huang D, Yuan J, *et al*. Multi-omics Biomarkers in Early Gastric Cancer Screening: Translating Discovery Evidence to Routine Screening Implementation. Cancer Screen Prev 2026;5(2):157–171. DOI: 10.14218/CSP.2026.00039.

[41] Leek JT, Scharpf RB, Bravo HC, Simcha D, Langmead B, Johnson WE, *et al*. Tackling the widespread and critical impact of batch effects in high-throughput data. Nat Rev Genet 2010;11(10):733–739. DOI: 10.1038/nrg2825, PMID: 20838408.